The Journal of Experimental Biology 211, 224-233
Published by The Company of Biologists 2008
doi:10.1242/jeb.007575

Review

When wings touch wakes: understanding locomotor force control by wake–wing interference in insect wings

Fritz-Olaf Lehmann
Biofuture Research Group, Institute of Neurobiology, University of Ulm, 89069 Ulm, Germany
e-mail: fritz.lehmann@uni-ulm.de

Accepted 21 May 2007

Summary

Understanding the fluid dynamics of force control in flying insects requires the exploration of how oscillating wings interact with the surrounding fluid. The production of vorticity and the shedding of vortical structures within the stroke cycle thus depend on two factors: the temporal structure of the flow induced by the wing's own instantaneous motion and the flow components resulting from both the force production in previous wing strokes and the motion of other wings flapping in close proximity. These wake–wing interactions may change on a stroke-by-stroke basis, confronting the neuro-muscular system of the animal with a complex problem for force control. In a single oscillating wing, the flow induced by the preceding half stroke may lower the wing's effective angle of attack but permits the recycling of kinetic energy from the wake *via* the wake capture mechanism. In two-winged insects, the acceleration fields produced by each wing may strongly interact *via* the clap-and-fling mechanism during the dorsal stroke reversal. Four-winged insects must cope with the fact that the flow over their hindwings is affected by the presence of the forewings. In these animals, a phase-shift between the stroke cycles of fore- and hindwing modulates aerodynamic performance of the hindwing *via* leading edge vortex destruction and changes in local flow condition including wake capture. Moreover, robotic wings demonstrate that phase-lag during peak performance and the strength of force modulation depend on the vertical spacing between the two stroke planes and the size ratio between fore- and hindwing. This study broadly summarizes the most prominent mechanisms of wake–wing and wing–wing interactions found in flapping insect wings and evaluates the consequences of these processes for the control of locomotor forces in the behaving animal.

Key words: wing–wing interaction, wake capture, clap-and-fling, LEV destruction, phase-shifted stroking, dragonfly, fruit fly, *Drosophila*.

Introduction

The extraordinary evolutionary success of flying insects is largely due to their ability to control locomotor behavior precisely in response to sensory stimuli. Numerous studies have emphasized the complexity of the feedback cascade that allows insects to convert sensory information, coming from the compound eyes, the gyroscopic halteres or the wing's campaniform sensilla, into locomotor activity (e.g. Dickinson and Palka, 1987; Egelhaaf and Borst, 1993; Kern et al., 2006; Nalbach, 1994; Sherman and Dickinson, 2004; Taylor, 2001). Behavioral performance may be limited at each step of this cascade, including the fluid dynamic processes with which flapping insect wings produce aerodynamic lift and drag. Force production and flight control in insects become most complex when fluid acceleration fields interfere with the flapping wings (Birch and Dickinson, 2003). Consequently, in a freely flying animal, the production of vorticity and shedding of vortical structures in each stroke cycle depend on several factors, such as (i) the instantaneous wake structure produced by the wing's own motion, (ii) wake components produced in a preceding half stroke or preceding stroke cycles, (iii) flow components resulting from force generation of wings flapping in close distance, (iv) changes in fluid velocity at the wings due to the animal's body motion along and around the three body axes and, finally, (v) external disturbances in the surrounding air. Taken together, these components determine the instantaneous flow regime around a flapping insect wing, and thus lift and drag production. To answer the question of how the neuro-muscular system of flying insects copes with changing fluid environments is intriguing and requires a deeper understanding of the fluid dynamic processes occurring in flapping insect wings (for reviews, see Lehmann, 2004; Sane, 2003).

In the past, the majority of studies on insect flight aerodynamics focused on the performance of single flapping wings and widely ignored the significance of wake patterns (wake history) produced by previous stroke cycles (e.g. Ellington, 1984). Fluid dynamic effects due to wake history, however, may be quite distinct, as demonstrated in a robotic *Drosophila* wing mimicking hovering conditions (Birch and Dickinson, 2001). In their study, Birch and Dickinson showed that the first stroke in a fruit fly model wing produces approximately 9% more lift than the subsequent strokes. The initial acceleration of the induced flow is responsible for this effect, because under the given experimental conditions induced flow may attenuate the wing's effective angle of attack by more than 10° (approximately 40° during first stroke cycle, 28–32° in subsequent cycles). The same kinematic pattern may also produce different amounts of lift due to the interaction of wakes produced by two flapping wings. The clap-and-fling mechanism that produces wake interferences between an ipsi- and contralateral wing and kinematic phase lag effects manipulating the flow regime between ipsilateral fore- and hindwings, are presumably the most

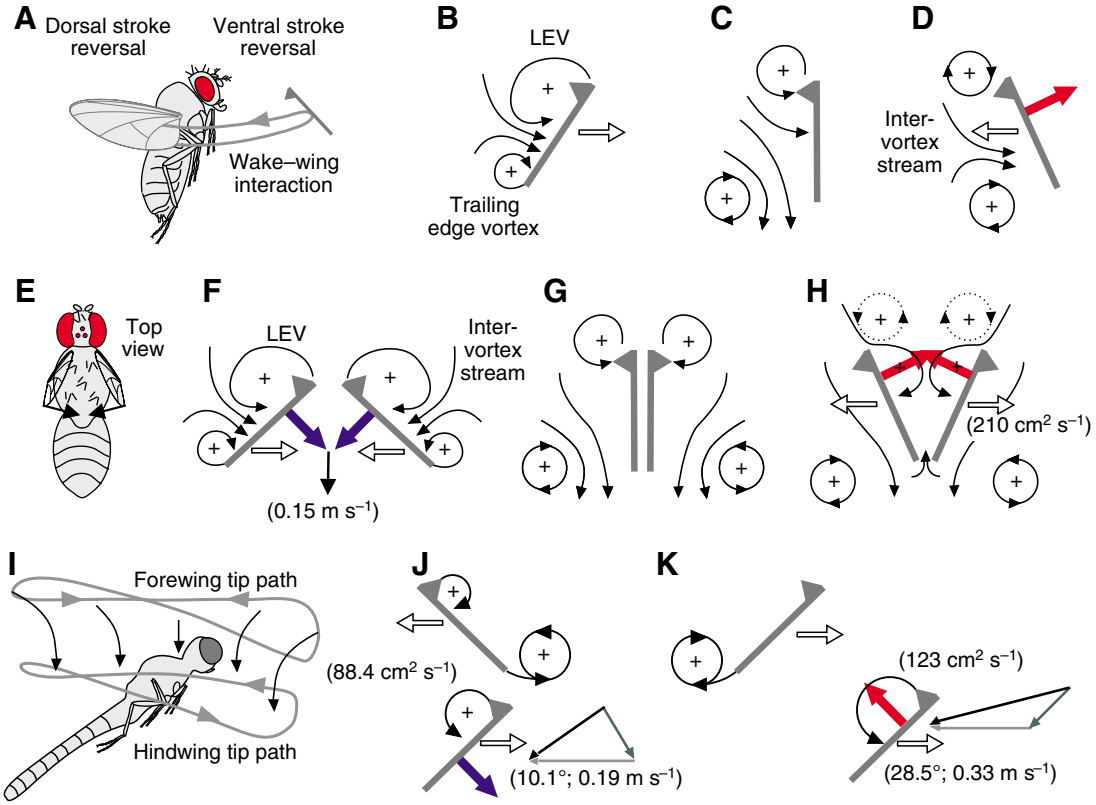

Fig. 1. Schematic reconstruction of wake pattern during wake–wing interaction in fruit fly and dragonfly model wings. (A–D) Wake capture mechanism at dorsal and ventral stroke reversal. At the beginning of each half stroke, the leading and trailing edge vortex system generates an inter-vortex stream towards the wing. (E–H) Schematic reconstruction of vortex generation and shedding during clap-and-fling maneuver using a generic *Drosophila* stroke kinematics (Lehmann et al., 2005). Chordwise wing segments at the end of the upstroke (F), during the clap phase (G), and during the fling phase (H) before the two wings separate for the downstroke. Leading and trailing edge vortices are shed into the wake at the end of each half stroke. The low-pressure region evolving between the wings during the fling pulls fluid around the leading and the trailing wing edge into the opening cleft. (I–K) Reconstruction of vortices and local flow conditions at maximum transient lift production in tandem model wings of a dragonfly. (I) Wing kinematics follows a generic pattern, as found in various species (Maybury and Lehmann, 2004). (J,K) Flow characteristics at 0.35 fraction of the stroke cycle at which either the fore- (upper wing; J) or the hindwing (lower wing; K) leads wing motion by a quarter stroke cycle. Local flow vector (black) in the vector diagrams is calculated from the velocity and angle of the combined fore–hindwing downwash (green vector) determined in a region below the hindwing's surface and the translational velocity of the hind wing section (gray vector). Effective angle of attack for the hind wing section (left value) and local flow velocity (right value) are shown, respectively, in parentheses below the vector diagram. Open arrows indicate the direction of wing motion. Vortical circulation in the hindwing's leading edge vortex (LEV) is shown in parentheses. The different strengths of starting and leading edge vortices are indicated approximately by the size of the plotted vortices. Blue and red arrows represent normalized vectors of total force attenuation and enhancement, respectively, compared to a wing flapping free from mirror- (F–H) and forewing (J,K) downwash. The exact inclination of the force vectors slightly differs from the orientation normal to the wing's surface, as shown in the schematics, because of shear forces in the fluid.

prominent examples of wake–wing interactions in flapping flight (Ellington, 1975; Maybury and Lehmann, 2004; Saharon and Luttges, 1989; Weis-Fogh, 1973).

Even within a single stroke cycle, a single wing may benefit from wake–wing interaction, namely at the beginning of each half stroke. This phenomenon is termed wake capture and describes a mechanism by which the animal extracts kinetic energy from the fluid (Fig. 1) (Dickinson et al., 1999; Srygley and Thomas, 2002). Wake capture at the beginning of the half stroke benefits from an inter-vortex stream produced by the leading and trailing edge vortex system that accelerates the fluid during wing rotation at the end of each half stroke (Birch and Dickinson, 2003) (Fig. 1A–D). However, this interpretation of wake capture force generation has been questioned by computational fluid dynamics (CFD) modeling of flapping insect wings, suggesting that the rotational-independent lift peak is due to a reaction of accelerating an added mass of fluid and does not rely on a momentum transfer of the fluid (Sun and Tang, 2002). In the past the effect of inertial reaction forces during the stroke reversals has been well recognized and discussed as a cause for wing rotation, twisting and bending (Daniel and Combes, 2002; Ennos, 1988a). For example, in two species of flies, the blowfly *Calliphora vicina* and the hoverfly *Eristalis tenax*, the high stroke frequency, ranging from 100 to 200 Hz, produces inertial forces sufficiently high to elicit passive wing pitch (angle of attack) changes when the wing reverses its direction of motion (Ennos, 1988b). Apart from this controversial view on the wake capture mechanism, it remains unclear how exactly the benefit of wake capture changes during fast forward or maneuvering flight of an insect when the wings experience additional fluid components produced by the animal's own body motion.

This study focuses on the most recent findings related to locomotor force control *via* wake–wing interaction in flapping insect wings and gives a broad summary of the fluid dynamic mechanisms underlying bilateral and ipsilateral wing–wing interference during hovering flight conditions. Novel data on the potential significance of (i) stroke plane distance between fore- and

hindwing and (ii) wing size, for fore- and hindwing lift production in an electromechanical dragonfly model during phase-shifted stroking are also presented. In a first set of experiments, the distance of both stroke planes was varied between 1.25 and 5 mean chord width of the hindwing in order to examine how changes in kinematic phase between the fore- and hindwing stroke cycles alter lift production. In a second set of experiments, the ratio of fore- to hindwing length was modified to explore (i) how these changes affect the phase between the two wings' beat cycles in which the wings generate maximum lift, and (ii) how the magnitude of peak-to-peak lift modulation alters with changing kinematic phase lag.

Dorsal wake–wing interference: the clap-and-fling mechanism

Wing kinematics at dorsal stroke reversal

The dorsal clap-and-fling mechanism in two- and four-winged insects was first described by Weis-Fogh (Weis-Fogh, 1973) and since then has been found in many insects with a vast variety of flight modes. It has been subjected to several detailed experimental evaluations. Quite recently, new approaches in experimental design have provided several new insights, and numerical modeling (CFD) has contributed much to our understanding of this particular kinematic maneuver.

The clap-and-fling is a close apposition of the ipsi- and contralateral wing at dorsal stroke reversal preceding pronation. During the clap, the insect brings the leading edges of the two wings together, then pronates them until the 'v-shaped' gap vanishes and the wings are parallel in close apposition. During the fling, the wings pronate about their trailing edges, creating a growing gap as the leading edge pulls apart (Fig. 1E–H). In Weis-Fog's classical reconstruction, the axis of wing rotation changes from rotation around the leading edge (upstroke) to a rotation around the trailing wing edge (downstroke) during pronation. This clap-and-fling kinematic pattern has been used for several experimental and numerical approaches (see below). Recent reconstructions of wing motion in tethered flight, however, have shown that during fling phase, the fruit fly *Drosophila virilis* apparently rotates its wings around the leading rather than the trailing wing edge. In rigid wings the latter maneuver would require that the wings be quickly pulled apart during rotation, whereas in the elastic wing of *Drosophila*, chordwise flexion permits the wings to rotate large angles of attack even at low gap angles (F.-O.L., manuscript in preparation). The latter kinematic pattern has previously been described as the 'peel' motion and found in several insects such as flies (Götz, 1987), butterflies (Brodsky, 1991), bush cricket (Brackenbury, 1990) and locust (Cooter and Baker, 1977). Preliminary two-dimensional digital particle image velocimetry (2D-DPIV) data on the wake structure of flying fruit flies during fling motion imply some fundamental fluid dynamic differences between rigid and elastic wings, particularly when considering the sign of circulation around the wings during pronation (F.-O.L., manuscript in preparation).

The fluid dynamic mechanisms of bilateral wake–wing interaction

The fling phase preceding the downstroke is thought to enhance circulation due to fluid inhalation in the cleft formed by the moving wings, causing strong vortex generation at the leading edge while the development of trailing edge vorticity is inhibited by trailing edge wing contact. Several studies have estimated the benefit of the fling part of wing motion, using either numerical models or a combined approach incorporating measurements of flow velocities and forces in robotic wings (e.g. Bennett, 1977; Edwards and Cheng, 1982; Ellington, 1975; Lighthill, 1973; Sunada et al., 1993). More recently, numerical simulations have been performed on the entire clap-and-fling sequence in both three dimensions (3D) (Sun and Yu, 2003) and two dimensions (2D) across a wide range of Reynolds numbers (Miller and Peskin, 2004). In addition, a dynamically scaled mechanical model of *Drosophila melanogaster* demonstrated that alteration in force production due to clap-and-fling wing motion is not limited to the dorsal stroke reversal but may also enhance lift approximately at mid downstroke and the beginning of the upstroke (Lehmann et al., 2005). Thus, clap-and-fling wing motion should be considered as a mechanism that may distort the spatio-temporal structure of the wake during up- and downstroke rather than affecting lift and drag production only in the brief moment during dorsal stroke reversal.

The strength of wake–wing interaction during clap-and-fling depends on several factors, including the thickness of the wing's boundary layer, as well as strength and direction of the induced flow during stroke reversal (Lighthill, 1973; Maxworthy, 1979). Experiments modifying the distance between the two rotating wings show that lift enhancement requires an angular separation between the two wings of no more than 10–12° (Reynolds number=134) (Lehmann et al., 2005). This value corresponds to a distance between the two rotational wing axes of approximately one mean wing chord of the *Drosophila* model wing. The relative benefit of clap-and-fling lift enhancement strongly depends on stroke kinematics. For example, insects that flap their wings with small stroke amplitudes should benefit relatively more from clap-and-fling force augmentation than insects that produce elevated flight forces by flapping their wings with stroke amplitudes close to the mechanical limit of the thoracic exoskeleton. In *Drosophila* model wings (160° stroke amplitude), maximum lift augmentation amounts to approximately 17% of the mean lift produced by a single wing flapping free from downwash of an image wing.

The time course of lift enhancement due to clap-and-fling is quite complex and consists of at least six distinct positive and negative force peaks. Two positive major force peaks are associated with wing motion during fling and a major negative peak occurs during the clap phase, in which lift and drag are transiently attenuated in the presence of an image wing. 2D-DPIV analysis has revealed that at this initial moment of dorsal wing–wing interaction, the local flow velocity at the wing's trailing edge is reduced by approximately 20%, compared to a single wing (Lehmann et al., 2005). Consequently, as the wings start the clap, the presence of an image wing diminishes the ability of each wing to accelerate fluid and thus generate aerodynamic forces. In other words, the presence of a contralateral image wing creates circulation of opposite sense very close to the ipsilateral wing that diminishes the ability of the wings to maintain circulation. Interestingly, this result is not confirmed by Sun's numerical model of the clap-and-fling (Sun and Yu, 2003). Their simulation suggests that, rather than an initial decrement, the wings in the two-wing case generate consistently higher force during wing motion preceding the clap than in the one-wing case.

During fling, force measurements yield two temporally transient positive peaks in lift and drag enhancement: (i) a large peak immediately after the wings start fling motion (0.08 of the stroke cycle), which accounts for most of the benefit in lift, and (ii) a second, smaller peak (0.20 of the stroke cycle), which enhances force at the end of the fling when the wings start to move apart. The DPIV images in Fig. 2B–E show the two leading edge vortices (LEV) in the opening cleft right before lift production peaks at early fling (0.05 of stroke cycle). Although at this time, circulation in the

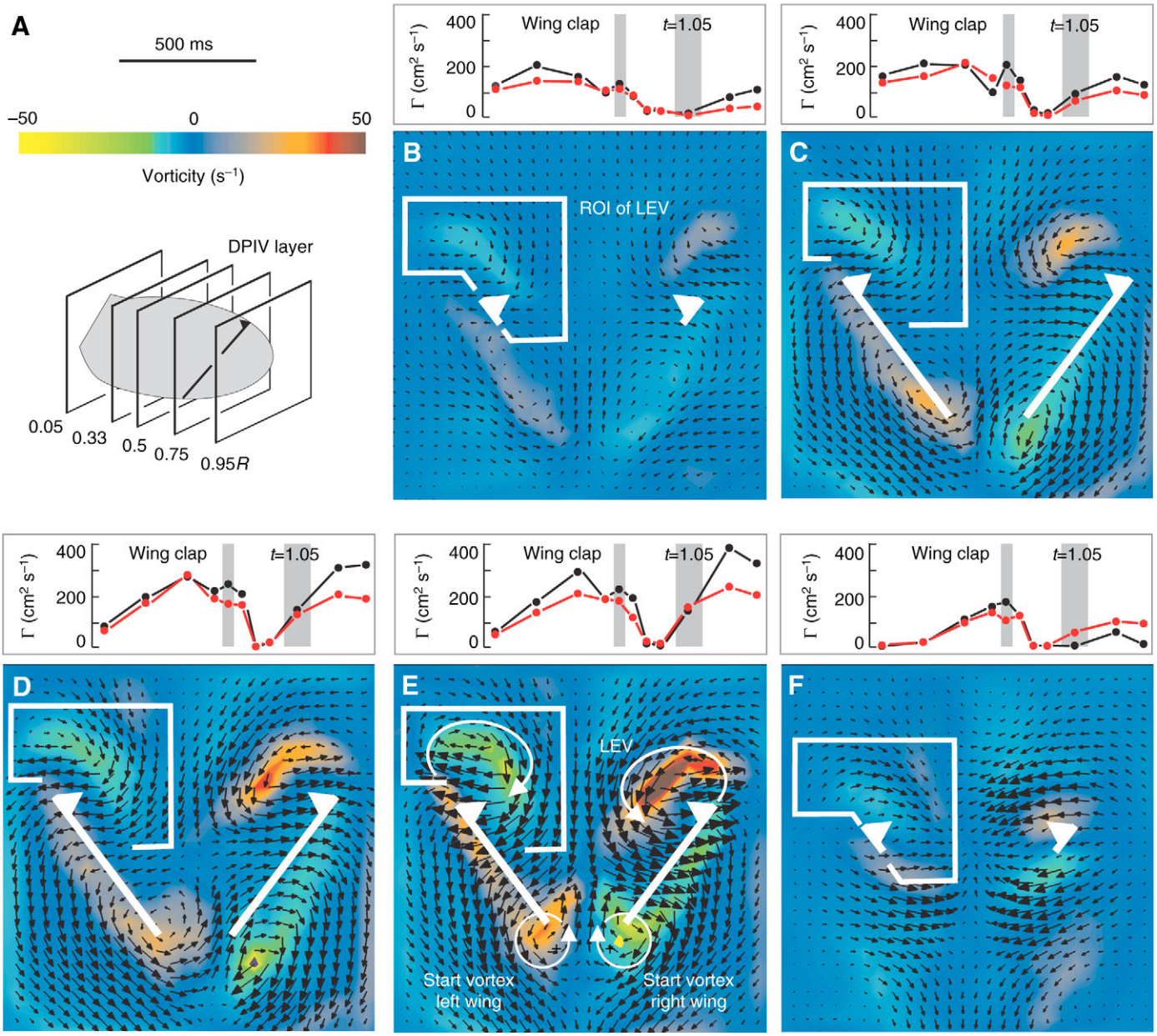

Fig. 2. Wake vorticity during fling phase in model *Drosophila* wings using 2D-DPIV analysis. The images were captured using a commercial 2D-DPIV system and a mini-Nd:YAG laser (TSI, Shoreview, MN, USA). (A) Wing shape and relative distance of five layers from the wing base used for analysis. Scale bar indicates time for the data traces in B–F. (B,C) Fluid vorticity fields at 0.05 stroke cycle after dorsal wing clap in a layer near the wing base (B), 0.33 (C), 0.5 (D), 0.75 wing length (E) and in a layer close to the wing tip (F). Data above each image show circulation Γ in the leading edge vortex (LEV), measured in a region of interest (ROI, white box). LEV circulation when flapping one and two wings are plotted in red and black, respectively. Gray bars in the graphs indicate wing clap and time at which the DPIV analysis was performed, respectively. White lines in panels indicate wing sections. The leading edge of the dorsal wing surface is indicated by a white triangle. The magnitude of vorticity is plotted in color code and arrows correspond to the magnitude of the velocity vector at each point in the fluid, longer arrows signify larger velocities. *t*=stroke cycle (0–1), *R*=wing length. See Lehmann et al. (Lehmann et al., 2005) for kinematics and further details on methods.

LEVs is not yet significantly larger than in a single wing (Fig. 2, white box and data traces; red, single wing; black, two wings), the translational velocity of the inflow into the opening cleft is significantly enhanced when flapping the ipsi- and contralateral wing (Fig. 2, length of black vectors). A possible explanation for the minor change in circulation of the LEV at this early state of the fling is fluid viscosity that acts against vortex induction. At low gap angles, circulation is significantly smaller than predicted by inviscid 2D numerical models, whereas circulation nearly matches the prediction at the late fling phase (Lighthill, 1973; Lehmann et al., 2005).

Moreover, it has been suggested that the biphasic character of fling-induced lift enhancement results from a transient inhibition of lift production due to the development of trailing edge vortices (Fig. 2C–E), rather than from distinct yet unknown fluid dynamic mechanisms. In contrast to Weis-Fogh's original model, wing separation in our robotic wing model allowed trailing edge vortices to form during the fling phase. The presence of trailing edge

vorticity, however, may inhibit the development of the LEV because fluid that is accelerated in the cleft from the rear potentially interferes with LEV induction (Fig. 1H, Fig. 2C–E). In elastic wings such as in *Drosophila*, the 'peel' offers a solution to that problem, because the tight contact between the trailing wing edges functions as a barrier to prevent fluid from being sucked into the opening cleft around the trailing edges.

Wake–wing interference between ipsilateral wings: dragonfly aerodynamics

Kinematic phase relationship

The third type of wake–wing interaction so far investigated is found in functionally four-winged insects such as dragon- and damselflies (Maybury and Lehmann, 2004; Reavis and Luttges, 1988; Saharon and Luttges, 1989; Somps and Luttges, 1985; Wang et al., 2003). The neuromuscular system allows these animals to actively change many aspects of wing motion in a single wing, such as the angle of attack, stroke plane, and more conventional parameters such as stroke amplitude and stroke frequency. Unlike four-winged insects with indirect flight musculature such as butterflies, bees, wasps and ants, however, dragon- and damselflies may actively control the timing between fore- and hindwing stroke cycles [the kinematic phase relationship (Norberg, 1975; Wakeling, 1993)]. In this respect, dragon- and damselflies even differ from other more primitive orders of functionally four-winged insects, such as locusts, in which phase relationship is highly consistent during flight with only little variation during steering maneuvers (Wortmann and Zarnack, 1993).

In general, dragonflies vary their phase relationship between ipsilateral fore- and hindwings with different behaviors. Behavioral studies on freely and tethered flying animals have reported three major categories of phase relationships: parallel stroking, counterstroking and phase-shifted stroking. During (i) straight forward and upward flight, (ii) escape behavior in which the animal produces peak lift of approximately 20 times its body weight and (iii) maneuvering flight, dragonflies typically use a conventional flight mode (Reavis and Luttges, 1988; Somps and Luttges, 1985; Wakeling and Ellington, 1997; Wang et al., 2003). A highly consistent characteristic for this flight mode is a 54–100° phase shift, during which the hindwing leads forewing motion. Larger phase differences of up to 180° (counterstroking) have been found in hovering dragonflies and maneuvering animals flying freely in a wind tunnel (Alexander, 1986).

Besides the changes in phase relationship between the two ipsilateral wings, dragonflies may employ two different gross types of wing motion: vertical and horizontal wing stroking. During vertical stroking, the animal's body is orientated approximately horizontally and both wing pairs beat in a vertical plane with high angle of attack during the downstroke and small angles of attack during the upstroke. During horizontal stroking, in contrast, the body is tilted upwards, as found in many other hovering insects and the wings beat approximately in a horizontal stroke plane (Fig. 1I) (Wakeling and Ellington, 1997). In this flight mode, the wing hinges of the fore- and hindwing are aligned approximately vertically and the wake produced by the forewings passes over the beating hindwings. Azuma et al. predicted that under those conditions, lift production of the hindwing should critically depend on the complex wake pattern produced by the beating wings, and thus on the fluid dynamic effects occurring during wing–wake interactions (Azuma et al., 1985). During maneuvering flight those complex interactions change, especially with transient changes in kinematic phase relationship, in which the relative timing of vortex shedding and fluid acceleration produced by the forewing changes with respect to hindwing aerodynamics.

Previous assumptions on wake–wing interaction in tandem wings

In previous studies on the aerodynamics of flying dragonflies (Alexander, 1986; Rüppell, 1989), it was suggested that in-phase, or parallel stroking, might produce higher aerodynamic forces than phase-shifted stroking or counterstroking. This conclusion was drawn from kinematic reconstructions of wing motion during the energetically most demanding flight modes such as hovering, take-off and load-lifting flight. Under these conditions, peak lift may increase by up to approximately 2.3–6.3 the times body weight when the animal decreases the phase angle between ipsilateral fore- and hindwing. However, the latter result apparently runs counter to previous numerical modelling (Lan, 1979). Lan's study predicts that the hindwing extracts maximum energy from the forewing downwash when the hindwing leads wing motion by a quarter stroke cycle. According to bi-plane theory, total lift production in tandem wings depends on the proximity and strength of forewing downwash that interferes with the hindwing (Milne-Thomson, 1966). Under such conditions, the hindwing must cope with a potential reduction in effective angle of attack and the interference between shed vorticity such as the forewing's start vortex and the hindwing's LEV. Since wake–wing interaction depends on forewing wake structure and the timing with which the hindwing interacts with the forewing wake, two long and narrow wings working independently should have higher lift-to-drag coefficients than a combined wing with the same area but different aspect ratio. In contrast to his later experimental findings, Alexander (Alexander, 1984) thus predicted that tandem wings flapping in-phase should produce less lift, because the two wings are always closer together than two wings flapping out-of-phase.

The impact of phase relationship on lift production in tandem wings

Dragonfly kinematics are very diverse, and various authors have modeled different types of dragonfly aerodynamics, employing both numerical and physical models (Kliss et al., 1989; Saharon and Luttges, 1988; Wang et al., 2004). More recently, Maybury and Lehmann (Maybury and Lehmann, 2004) used a fully computer-controlled robotic wing (electromechanical flapper) and performed direct force measurements on the wing hinge, including measurements on the wake structure, using 2D-DPIV, Fig. 3A,D). While varying the phase relationship between the two horizontally beating wings, the authors showed how the performance of the fore- and hindwing varies in response to kinematic phase-shifting (Fig. 4A,B). The most unexpected result in this research was that the hindwing regains aerodynamic performance close to that of a wing without forewing interference, when the motion of the hindwing leads the forewing by approximately a quarter stroke cycle. When the forewing leads wing motion by a quarter stroke cycle, hindwing lift production decreases by approximately 40% compared to a single wing. The approximately twofold change in aerodynamic performance of the hindwing follows a sinusoidal curve when phase relationship linearly changes from –50% (forewing leads wing motion) to 50% stroke cycle (hindwing leads wing motion, counterstroking, Fig. 4B). This relationship implies that small changes in phase lag around –25% and 25% stroke cycle only produce moderate changes in hindwing lift production, whereas in parallel stroking,

the same phase alterations produce considerable larger modulations in hindwing lift.

The reconstruction of vorticity in the vortical structures and velocity measurements of the oncoming fluid suggest two distinct fluid dynamic phenomena for hindwing lift modulation. First, the destruction of the leading edge vortex due to the proximity of the forewing's starting vortex and, second, the changes in strength and orientation of the local flow vector. When the forewing leads wing motion by a quarter stroke cycle, both the forewing's start vortex and induced flow negatively affect the hindwing's LEV and effective angle of attack throughout the stroke cycle, respectively (Fig. 3B for 0.15 stroke cycle; Fig. 1J for 0.35 stroke cycle). The same holds true for the initial part in each half stroke (0–0.15 stroke cycle) when the hindwing leads wing motion by a quarter stroke cycle. In the latter case, however, the hindwing regains instantaneous lift in excess of the instantaneous lift produced by a single flapping wing during the second half of each half stroke. This effect occurs because the hindwing's LEV development is not hindered by the proximity of the forewing's start vortex when the wing additionally gains lift by the wake capture mechanisms. The

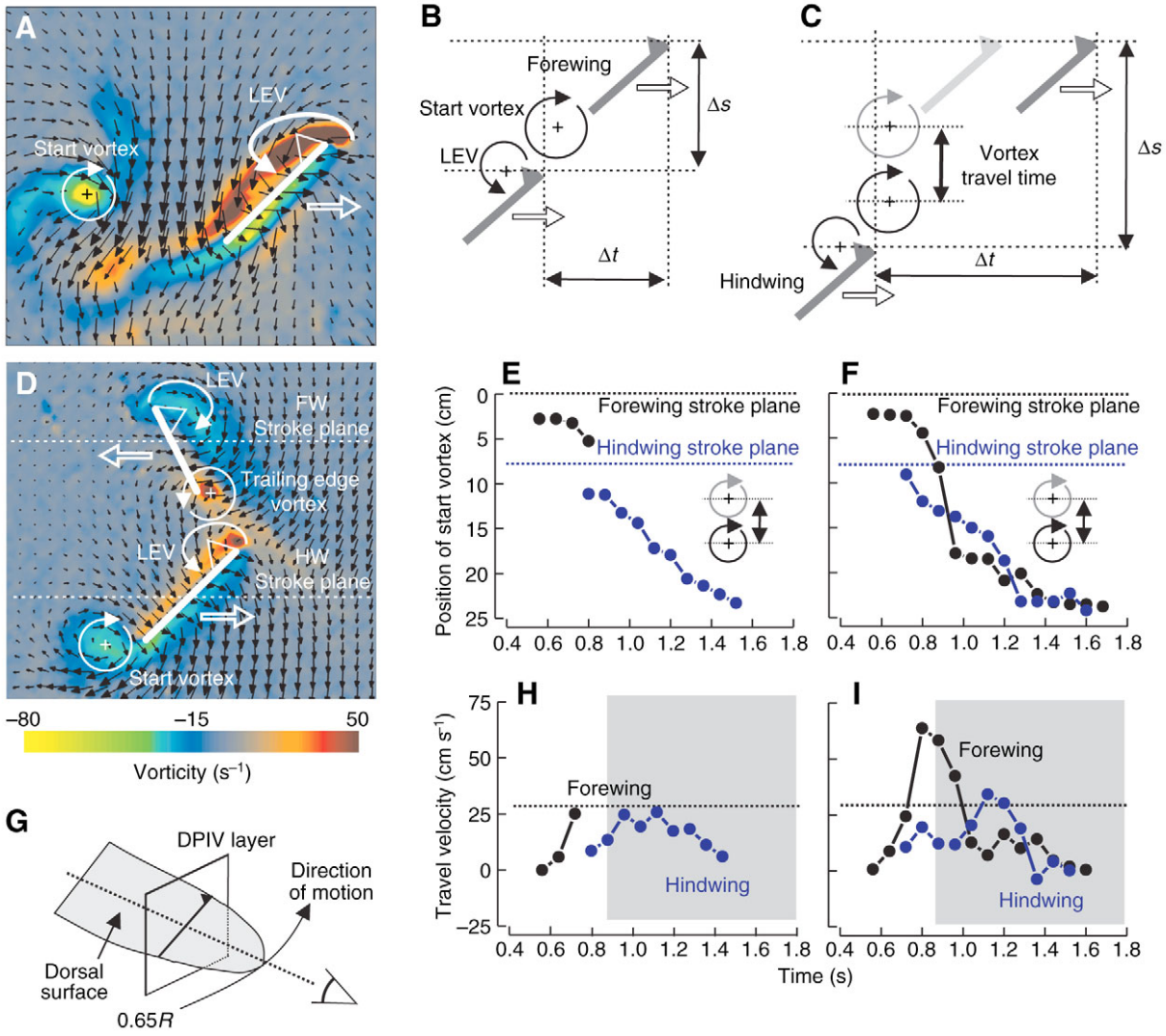

Fig. 3. Mean lift production in dragonfly model wings depends on both the phase-shift between fore- and hindwing stroke cycle and the vertical separation between the two wing hinges. (A) Vortical structures produced by a dragonfly hindwing at 0.35 hindwing stroke cycle. The wing moves from left to right (open arrow). The wing blade element that runs through the center of force at 0.65 wing length is indicated by a white line and the leading edge is indicated by a triangle, as shown in G. Inclination and length of the black vectors indicate direction and relative magnitude of fluid velocity. (B,C) Schematic explanation of how vertical spacing (Δs) between fore- and hindwing stroke plane changes kinematic phase relationship between both wings (Δt) due to vortex travel time at 0.35 stroke cycle. When the forewing leads wing motion, destruction of hindwing LEV by the forewing's start vortex depends on the phase-shift between both stroke cycles and the vertical distance between both ipsilateral wing hinges. (D) DPIV image showing the interference between vortical structures produced by fore- and hindwing at 0.15 hindwing stroke cycle. The hindwing leads wing motion by 0.25 stroke cycle. While the forewing (upper blade element) starts wing rotation at the end of the downstroke, its trailing edge vortex interferes with the LEV produced by the hindwing (lower blade element). The hindwing's start vortex still appears to be attached to the wing's trailing edge. (E,F,H,I) Vertical position (E,F) and vertical travel velocity of start vortices (H,I) shed from the fore- (black) and hindwing (blue). The vortex positions were only reconstructed from flow images in which the vortical structures were clearly visible. The data are recorded while the forewing (E,H) and the hindwing (F,I) was leading wing motion by a quarter stroke cycle, respectively. Shaded areas in H and I indicate the period during which the forewing start vortex interferes with the hindwing wake, and the dotted lines indicate maximum downwash velocity measured in the hindwing wake. *R*=wing length, LEV=leading edge vortex, HW=hindwing, FW=forewing.

DPIV measurements revealed that the enhanced wake capture effect is caused by the favorable orientation of the forewing downwash. At 0.35 stroke cycle, forewing downwash increases the hindwing's effective angle of attack by 31% (from approximately 20° in a single wing to 28.5° in two wings) and reinforces local flow velocity by 43% (from 0.19 to 0.33 m s^{-1}; Fig. 1K, black vector). Consequently, despite the unfavorable effect of the forewing wake on the hindwing's LEV in the early part of the stroke, a hindwing beating with a 25% phase lag relative to the forewing can achieve the same mean lift as a single wing due to wake capture.

The modulation effects in aerodynamic performance due to kinematic phase relationship are not restricted to the hindwing but also produce considerable changes in lift production of the forewing. Although those changes are smaller and only occur in phase-shift cases where fore- and hindwings were moving close to each other (blue line, Fig. 4A), combined lift of both wings varies accordingly. It seems likely that some of the modulations in forewing lift are caused by the wall effect due to the physical distortion of the forewing downwash by the hindwing. Previous work predicted maximum increase in forewing lift when the forewing downwash is directed completely onto the dorsal surface of the hindwing throughout the stroke cycle (Rayner, 1991). At a vertical distance of 1.25 wing chord between both stroke planes, this situation occurs when the forewing leads wing motion by approximately 2.5–5%, whereas forewing lift is significantly diminished when the hindwing leads wing motion (Fig. 4A).

Vortex travel time

Although the above findings may enable functionally four-winged insects to control ipsilateral flight force without further changes in wing beat kinematics, phase lag at peak performance should critically depend on (i) the animal's flight speed and thus reduced frequency, (ii) the vertical distance between the two wing hinges and (iii) shape and size of the fore- and hindwing. While wing size determines downwash strength and spatial shape of the wake (cf. below), flight speed and vertical wing separation affect travel time of vortical structures shed from the forewing, until they interfere with hindwing motion. To understand the fluid dynamic consequences of vertical wing spacing in more detail, we reconstructed the vertical position of start vortices shed by the two wings from our DPIV data (Fig. 3E,F) and calculated the travel velocity from vortex positions in 12 subsequent, temporally equally spaced images (0.08 s spacing; Fig. 3H,I). The analysis reveals that the travel velocity of the hindwing start vortices reaches peak values of approximately 25 cm s^{-1} and appears to be broadly independent on the phase lag between fore- and hindwing stroke cycle. The forewing's start vortices, in contrast, transiently achieve much higher travel velocities of up to 60 cm s^{-1}, close to the hindwing stroke plane. A most likely explanation of this phenomenon is that the two wings produce an elevated pressure gradient in the space between both stroke planes. Thus, a vortex passing through that space might experience higher accelerations compared to a vortex shed by a single flapping wing. It must remain open, however, whether the pronounced acceleration of the forewing start vortices is limited to flapping conditions in which the hindwing leads wing motion by 25% stroke cycle (Fig. 3I), because it was almost impossible to detect the forewing's start vortices in the hindwing wake when the forewing leads wing motion by 25% stroke cycle (Fig. 3H).

The consequences of increasing the vertical spacing between the two wing hinges of the dragonfly model are twofold. First, an increasing vertical spacing should attenuate the amplitude of modulation in fore- and hindwing lift, because fluid viscosity smoothes out temporal fluctuations in the wake. The required distance between fore- and hindwing to avoid lift fluctuations in response to phase-shifting depends on both the strength of induced flow and fluid viscosity, and thus on Reynolds number. At an intermediate Reynolds number of our model wings (Re=105–125), the data show that force modulation of the hindwing ceases when both wing hinges are separated by at least five mean chord widths, i.e. approximately 20 cm. Since wall effects on the forewing are absent at this spacing, the forewing, in this case, produces lift similar to the performance of a single

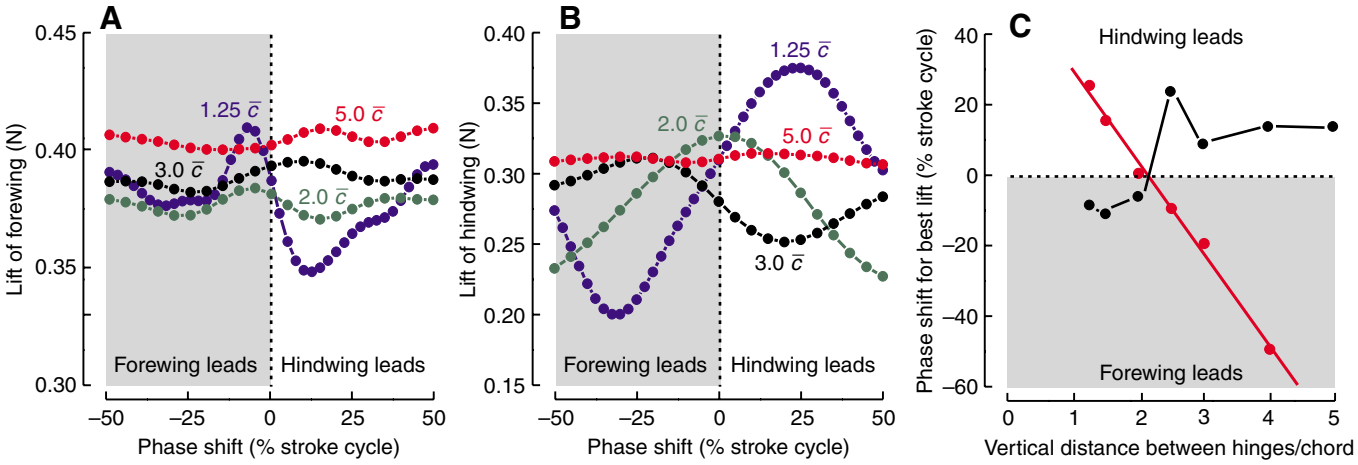

Fig. 4. Modulation of lift with changing phase-shift between the stroke cycles of dragonfly tandem wings. (A,B) Data show modulation of forewing (A) and hindwing (B) lift averaged over the entire flapping cycles of four subsequent strokes, while phase lag systematically varied between –50% (forewing lead by a half stroke cycle) and 50% (hindwing leads by a half stroke cycle). Colors show measurements at different vertical distances between the stroke planes (1.25 to 5 mean wing chord $\bar{c}$). (C) Phase-shift between the stroke cycles of both wings during mean peak lift changes with changing vertical distance between the two wing hinges. Black, forewing; red, hindwing; aspect ratio of the wings=2.7; flapping frequency=666 mHz; wing rotation symmetrical, starting 10% prior to and ending 10% after stroke reversal; Reynolds number=137; $\bar{c}$=4.0 cm. Data in A and B were smoothed using a numerical 3 data point adjacent averaging filter.

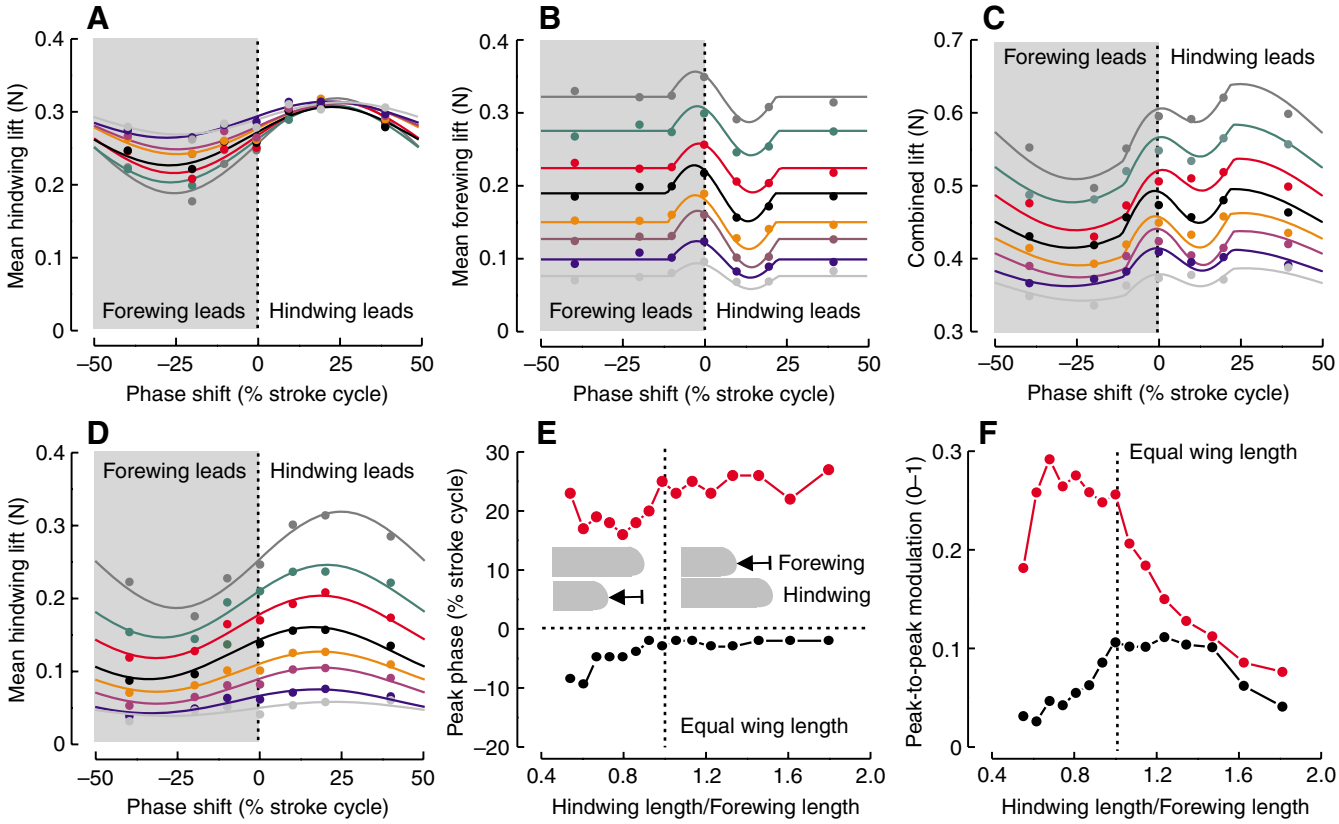

Fig. 5. Phase-shift induced modulation of mean lift production depends on wing length in tandem model wings. The length of the model wings was 6.9 (light gray), 7.7 (blue), 8.5 (purple), 9.3 (orange), 10.1 (black), 10.9 (red), 11.7 (green) and 12.5 cm (dark gray). (A) Lift modulation of the lower hindwing (12.5 cm wing length), while length of the upper forewing varied between 6.9 and 12.5 cm. (B) Lift modulation in length-changing forewing and length constant hindwing of 12.5 cm. (C) Combined fore- and hindwing lift as shown in A and B, respectively. (D) Hindwing lift modulation during length changes of the hindwing. Forewing length is constant at 12.5 cm. (E) Peak phase at which fore- (black) and hindwing (red) produce maximum mean lift. Data are plotted against the ratio between hind- and forewing length. A value of 1.0 means that both wings have equal length (12.5 cm). (F) Strength of peak-to-peak modulation of fore- (black) and hindwing (red) lift production. Modulations were derived from sinusoidal fits to the data set (forewing lift: fit on data between ±15% phase-shift, hindwing lift: fit on all data) as shown by the colors in A–D. Insets in E show the shape of the model wings used in the experiments. The rounded wing tip was similar in all wings while total wing length varied between minimum and maximum values. Aspect ratio varied between approximately 1.7 (6.9 cm wing length) and 3.1 (12.5 cm wing length), respectively. Wing chord=4.0 cm. Vertical distance between both wings was 1.25 mean wing chord. For kinematic pattern, see legend of Fig. 4. More information on the methods is given elsewhere (Maybury and Lehmann, 2004).

wing (Fig. 4A, red). However, the hindwing is still affected by the uniform forewing downwash and thus generates approximately 15% less lift than a single wing flapping free of forewing downwash (Fig. 4B, red). Second, the quarter-stroke cycle phase lag (25%), at which the hindwing achieves maximum mean lift when stroke planes are closest, should decrease with increasing distance between the stroke planes because of an increase in vortex travel time. This relationship may be demonstrated by plotting kinematic phase lag at peak lift production as a function of the vertical distance between both wing hinges (Fig. 4C). As expected from the significance of forewing start vortices for wake–wing interaction of the hindwing, the data show that kinematic phase lag for maximum hindwing lift (Fig. 4C, red) linearly decreases from 25% to –50% stroke cycle with increasing wing separation (linear regression fit, y=55.3–26.1x, N=6, R^2=0.99, P<0.0001), whereas phase lag for forewing lift (Fig. 4C, black) tends to increase with increasing distance (linear regression fit, P=0.09). Within the limits of our experimental approach, this finding eventually means that in-phase, or parallel, stroking produces maximum hindwing lift only when the two stroke planes are separated by approximately two mean wing chords – a value that is well above the value typically found in dragon- and damselflies.

The significance of wing shape for lift modulation in tandem wings

In many dragon- and damselflies, fore- and hindwings have different sizes and thus contribute different amounts of lift to total aerodynamic performance, assuming similar stroke kinematics. It is difficult to predict the significance of these morphological adaptations for dragonfly aerodynamics from the previous results, because local flow conditions at both wings depend on the complex interaction between fore- and hindwing wakes. For example, a short forewing is likely to attenuate lift modulation in the hindwing because of the reduced magnitude in downwash. A longer hindwing, in turn, might pick up more of the forewing's downwash, yielding an increase in phase-dependent lift modulation. We investigated this problem experimentally by replacing the dragonfly model wings of the electromechanical flapper by a set of generic wings with rounded tips (Fig. 5E). While the shape of the wing tip was identical in all tested wings, we varied the length of the fore- and hindwings in eight steps in order to obtain equally

spaced aspect ratios (length, aspect ratio: 6.9 cm, 1.7; 7.7, 1.9; 8.5, 2.1; 9.3, 2.3; 10.1, 2.5; 10.9, 2.7; 11.7, 2.9 and 12.5, 3.1). Similar to the experiments in Fig. 4, the kinematic pattern was a generic pattern developed for hovering dragonflies (Maybury and Lehmann, 2004).

The measurements show that the amplitude of modulation in hindwing lift strongly depends on the size ratio between fore- and hindwing. At maximum hindwing length (aspect ratio=3.1), modulation in hindwing lift decreases with decreasing forewing length while maximum lift at 25% phase-shift remains approximately unchanged (Fig. 5A). In contrast, at maximum forewing length (aspect ratio=3.1), maximum hindwing lift decreases with decreasing hindwing length due to the decreasing wing area (Fig. 5D). Compared to the hindwing, the changes in peak-to-peak amplitude of modulation in forewing lift are less pronounced and limited to a small window of approximately ±15% phase lag (Fig. 5B). Consequently, the combined lift of both wings shows two characteristic positive peaks: a smaller peak during parallel stroking (0% phase lag) due to the wall effect on the forewing and a larger lift peak during phase-shifted stroking (25% phase lag) due to beneficial wake capture of the hindwing (Fig. 5C). Most notably, kinematic phase at mean peak lift slightly increases with increasing hindwing/forewing size ratio in the forewing (linear regression fit, y=–9.13+4.97x, N=16, R^2=0.54, P=0.0013; Fig. 5E, black) and the hindwing (linear regression fit, y=15.1+6.66x, N=16, R^2=0.46, P=0.004; Fig. 5E, red).

In contrast to the comparatively small changes in peak phase, the modulation of lift varies considerably at different wing size ratios (Fig. 5F). Although vertical distance between both wings was identical in all experiments (1.25 mean wing chord), the data expose a complex dependency of peak-to-peak modulation from size ratio that can be broadly summarized as follows: At length ratios of between 0.7 and 1.0, hindwing lift modulation (Fig. 5F, red) changes only little, whereas forewing modulation (Fig. 4F, black) tends to increase with increasing size ratio. At length ratios of between 1.0 and 1.5, in contrast, forewing lift modulation changes only little, but hindwing lift modulation sharply decreases with increasing wing length ratio. Thus, when insects change the phase lag between fore- and hindwing to modulate the total amount of generated lift, this modulation might be affected by the ratio of fore- and hindwing length. Consequently, in dragon- and damselflies with long fore- and short hindwings (length ratios 0.6–1.0) changes in phase lag mainly modulate how much lift is generated by the hindwings, while in insects with short fore- and long hindwings (length ratio 1.0–1.5), both wings might experience significant modulations of their mean lift.

Concluding remarks

Wing–wing and wake–wing interactions in flapping insect wings permit flying animals to modulate their flight forces due to comparatively complex fluid dynamic processes. Bilateral wing–wing interaction (clap-and-fling), for example in *Drosophila*, requires only small changes in dorsal wing stroke angle of no more than 12° in order to modulate total lift of up to approximately 17%, compared to a single wing. Changes in kinematic phase lag between ipsilateral fore- and hindwings might enable dragonflies and other functionally four-winged insect to modulate lift by a factor of two without further changes in stroke kinematics. In this context, it has been suggested that wake–wing induced changes in instantaneous lift and drag might also favor the control of moments around the animal's roll, pitch and yaw body axes. Since the clap-and-fling in *Drosophila* mainly causes lift at the dorsal stroke reversal, it produces nose-down pitching moments that conveniently counterbalance nose-up pitching moments due to an increase in ventral stroke amplitude (Lehmann et al., 2005). Although this mechanism might help an animal to stabilize its body posture during flight, the situation is more complex because kinematic patterns that produce similar fling-induced mean lift and drag augmentation may produce different amounts of pitching moments (Lehmann and Pick, 2007). Moreover, even if we assume that lift and drag modulations due to wing–wake interaction may be high enough to sufficiently serve the insect as a tool to control its flight performance, it still remains an unproven hypothesis whether the insect's neuromuscular system can control these complex interactions to use them for flight control. An alternative concept would thus be to consider wake–wing interactions simply as an unavoidable effect that insects have to deal with during flight. In this case, the contribution of wake–wing interactions to forces and moments renders mute the issue of any possible irrelevance for insect flight control. Eventually, even though robotic experiments would find some inherently uncontrollable fluid dynamic interactions between two beating wings, then those studies might teach us which kinematic patterns insects should avoid at all costs, or have yet to exploit to make their flight behavior erratic.

I would like to thank Ursula Seifert for critically reading an early version of this manuscript. The presented work was funded by a German Federal Ministry for Education and Research (BMBF) grant Biofuture 0311885 and a German Science Foundation grant Le905/8-1.

References

Alexander, D. E. (1984). Unusual phase relationships between the forewings and hindwings in flying dragonflies. *J. Exp. Biol.* **109**, 379-383.
Alexander, D. E. (1986). Wind tunnel studies of turns by flying dragonflies. *J. Exp. Biol.* **122**, 81-98.
Azuma, A., Azuma, S., Watanabe, I. and Furuta, T. (1985). Flight mechanics of a dragonfly. *J. Exp. Biol.* **116**, 79-107.
Bennett, L. (1977). Clap and fling aerodynamics: an experimental evaluation. *J. Exp. Biol.* **69**, 261-272.
Birch, J. M. and Dickinson, M. H. (2001). Spanwise flow and the attachment of the leading-edge vortex on insect wings. *Nature* **412**, 729-733.
Birch, J. M. and Dickinson, M. H. (2003). The influence of wake–wing interactions on the production of aerodynamic forces in flapping flight. *J. Exp. Biol.* **206**, 2257-2272.
Brackenbury, J. (1990). Wing movements in the bush cricket *Tettigonia viridissima* and the mantis *Ameles spallanziana* during natural leaping. *J. Zool. Lond.* **220**, 593-602.
Brodsky, A. K. (1991). Vortex formation in the tethered flight of the peacock butterfly *Inachis io* L. (Lepidoptera, Nymphalidae) and some aspects of insect flight evolution. *J. Exp. Biol.* **161**, 77-95.
Cooter, R. J. and Baker, P. S. (1977). Weis-Fogh clap and fling mechanism in *Locusta*. *Nature* **269**, 53-54.
Daniel, T. L. and Combes, S. A. (2002). Flexible wings and fins: bending by inertial or fluid-dynamic forces? *Int. Comp. Biol.* **42**, 1044-1049.
Dickinson, M. H. and Palka, J. (1987). Physiological properties, time of development, and central projection are correlated in the wing mechanoreceptors of *Drosophila*. *J. Neurosci.* **7**, 4201-4208.
Dickinson, M. H., Lehmann, F.-O. and Sane, S. (1999). Wing rotation and the aerodynamic basis of insect flight. *Science* **284**, 1954-1960.
Edwards, R. H. and Cheng, H. K. (1982). The separation vortex in the Weis-Fogh circulation-generation mechanism. *J. Fluid Mech.* **120**, 463-473.
Egelhaaf, M. and Borst, A. (1993). Motion computation and visual orientation in flies. *Comp. Biochem. Physiol.* **104A,** 659-673.
Ellington, C. P. (1975). Non-steady-state aerodynamics of the flight of *Encarsia formosa*. In *Swimming and Flying in Nature*. Vol. 2 (ed. T. Y. Wu, C. J. Brokaw and C. Brennen), pp. 783-796. New York: Plenum Press.
Ellington, C. P. (1984). The aerodynamics of hovering insect flight. *Philos. Trans. R. Soc. Lond. B Biol. Sci.* **305**, 1-181.
Ennos, A. R. (1988a). The importance of torsion in the design of insect wings. *J. Exp. Biol.* **140**, 137-160.
Ennos, A. R. (1988b). The inertial cause of wing rotation in Diptera. *J. Exp. Biol.* **140**, 161-169.
Götz, K. G. (1987). Course-control, metabolism and wing interference during ultralong tethered flight in *Drosophila melanogaster*. *J. Exp. Biol.* **128**, 35-46.
Kern, R., van Hateren, J. H. and Egelhaaf, M. (2006). Representation of behaviourally relevant information by blowfly motion-sensitive visual interneurons requires precise compensatory head movements. *J. Exp. Biol.* **209**, 1251-1260.
Kliss, M., Somps, C. and Luttges, M. W. (1989). Stable vortex structures: a flat plate model of dragonfly hovering. *J. Theor. Biol.* **136**, 209-228.

Lan, C. E. (1979). The unsteady quasi-vortex-lattice method with applications to animal propulsion. *J. Fluid Mech.* **93**, 747-765.
Lehmann, F.-O. (2004). The mechanisms of lift enhancement in insect flight. *Naturwissenschaften* **91**, 101-122.
Lehmann, F.-O. and Pick, S. (2007). The aerodynamic benefit of wing–wing interaction depends on stroke trajectory in flapping insect wings. *J. Exp. Biol.* **210**, 1362-1377.
Lehmann, F. O., Sane, S. P. and Dickinson, M. H. (2005). The aerodynamic effects of wing–wing interaction in flapping insect wings. *J. Exp. Biol.* **208**, 3075-3092.
Lighthill, M. J. (1973). On the Weis-Fogh mechanism of lift generation. *J. Fluid Mech.* **60**, 1-17.
Maxworthy, T. (1979). Experiments on the Weis-Fogh mechanism of lift generation by insects in hovering flight. Part 1. Dynamics of the 'fling'. *J. Fluid Mech.* **93**, 47-63.
Maybury, W. J. and Lehmann, F.-O. (2004). The fluid dynamics of flight control by kinematic phase lag variation between two robotic insect wings. *J. Exp. Biol.* **207**, 4707-4726.
Miller, L. A. and Peskin, C. S. (2004). When vortices stick: an aerodynamic transition in tiny insect flight. *J. Exp. Biol.* **207**, 3073-3088.
Milne-Thomson, L. M. (1966). *Theoretical Aerodynamics*. New York: Macmillan.
Nalbach, G. (1994). Extremely non-orthogonal axes in a sense organ for rotation: behavioral analysis of the dipteran haltere system. *Neuroscience* **61**, 149-163.
Norberg, R. A. (1975). Hovering flight of the dragonfly *Aeschna juncea* L. In *Kinematics and Aerodynamics*. Vol. 2 (ed. T. Y.-T. Wu, C. J. Brokaw and C. Brennen), pp. 763-781. New York: Plenum Press.
Rayner, J. M. V. (1991). On the aerodynamics of animal flight in ground effect. *Philos. Trans. R. Soc. Lond. B Biol. Sci.* **334**, 119-128.
Reavis, M. A. and Luttges, M. W. (1988). Aerodynamic forces produced by a dragonfly. *AIAA J.* **88-0330**, 1-13.
Rüppell, G. (1989). Kinematic analysis of symmetrical flight manoeuvres of odonata. *J. Exp. Biol.* **144**, 13-42.
Saharon, D. and Luttges, M. W. (1988). Visualization of unsteady separated flow produces by mechanically driven dragonfly wing kinematics model. *AIAA J.* **88-0569**, 1-23.
Saharon, D. and Luttges, M. W. (1989). Dragonfly unsteady aerodynamics: the role of the wing phase relationship in controlling the produced flows. *AIAA J.* **89-0832**, 1-19.
Sane, S. (2003). The aerodynamics of insect flight. *J. Exp. Biol.* **206**, 4191-4208.
Sherman, A. and Dickinson, M. H. (2004). Summation of visual and mechanosensory feedback in *Drosophila* flight control. *J. Exp. Biol.* **207**, 133-142.
Somps, C. and Luttges, M. (1985). Dragonfly flight: novel uses of unsteady separated flows. *Science* **228**, 1326-1329.
Srygley, R. B. and Thomas, A. L. R. (2002). Unconventional lift-generating mechanisms in free-flying butterflies. *Nature* **420**, 660-664.
Sun, M. and Tang, J. (2002). Lift and power requirements of hovering flight in *Drosophila virilis*. *J. Exp. Biol.* **205**, 2413-2427.
Sun, M. and Yu, X. (2003). Flows around two airfoils performing fling and subsequent translation and translation and subsequent clap. *Acta Mech. Sin.* **19**, 103-117.
Sunada, S., Kawachi, K., Watanabe, I. and Azuma, A. (1993). Fundamental analysis of three-dimensional 'near fling'. *J. Exp. Biol.* **183**, 217-248.
Taylor, G. K. (2001). Mechanics and aerodynamics of insect flight control. *Biol. Rev.* **76**, 449-471.
Wakeling, J. M. (1993). Dragonfly aerodynamics and unsteady mechanisms: a review. *Odonatologica* **22**, 319-334.
Wakeling, J. M. and Ellington, C. P. (1997). Dragonfly flight II. Velocities, accelerations, and kinematics of flapping flight. *J. Exp. Biol.* **200**, 557-582.
Wang, H., Zeng, L., Liu, H. and Chunyong, Y. (2003). Measuring wing kinematics, flight trajectory and body attitude during forward flight and turning maneuvers in dragonflies. *J. Exp. Biol.* **206**, 745-757.
Wang, Z. J., Birch, J. M. and Dickinson, M. H. (2004). Unsteady forces and flows in low Reynolds number hovering flight: two dimensional computation *vs* robotic wing experiments. *J. Exp. Biol.* **207**, 449-460.
Weis-Fogh, T. (1973). Quick estimates of flight fitness in hovering animals, including novel mechanisms for lift production. *J. Exp. Biol.* **59**, 169-230.
Wortmann, M. and Zarnack, W. (1993). Wing movements and lift regulation in the flight of desert locusts. *J. Exp. Biol.* **182**, 57-69.